Supporting Information

Tsvetkov et al. 10.1073/pnas.1004498107

SI Materials and Methods

Plasmids and Chemicals. Bafilomycin A, rapamycin, trifluoroperazine, promazine, triflupromazine, chlorpromazine, mesoridazine, promethazine, nortriptyline, phenoxazine, phenothiazine, quinacrine, loperamide, pimozide, niguldipine, fluspirilene, and actin antibody were from Sigma. Everolimus was from Walter Schuler (Novartis; Basel, Switzerland). Thioridazine was from MP Biomedicals. Akt inhibitors V, VII, IX, and 10-NCP were from Calbiochem. Previously described antibodies against LC3 (1) were from Dr. Debnath (University of California, San Francisco), or from MBL International and were then developed in our laboratory. Antibodies against Akt, phospho-Akt (Ser473), mTOR, phospho-mTOR (Ser2448), p70S6K, and phospho-p70S6K (Thr389) were from Cell Signaling. Antibody 3B5H10 was from Sigma. BDNF was from Amgen. mCherry, a gift from R. Tsien (University of California, San Diego), was cloned into the pGW1 vector. pGW1-GFP and pGW1-Htt^{ex1}-Q72-GFP were as described by Arrasate et al. (2).

Cell Cultures. HeLa cells were cultured in DMEM with 10% FBS (HyClone) and treated 24 h after plating.

Striata, cortices, and hippocampi from rat embryos (embryo days 17–18) were dissected, dissociated, and plated on 24-well tissue culture plates (0.7×10^6 per well) coated with poly-D-lysine and laminin, as described (2–4). Cells were cultured for 7–10 d in neurobasal medium with L-glutamine and B-27 before use.

Striata from newborn (postnatal day 0) mice transgenic for GFP-LC3 (5) were plated on poly-D-lysine–coated 24-well tissue culture plates at $0.2–0.7 \times 10^6$ per well. Certain experiments were performed 24 h after transfection with Lipofectamine 2000 (Invitrogen).

R6/2 ovarian transplant female mice were from the Jackson Laboratory. Striata from newborn R6/2 mice were cultured as GFP-LC3 mouse neurons. At 7 d in vitro, neurons were treated overnight with 0.5, 1, or 5 μM 10-NCP.

Treatments. In most studies, neurons were treated with 1–10 nM bafilomycin A for 4–6 h, 1–10 μM 10-NCP for 4–168 h; with 100 ng/mL BDNF, 5 μM Akt inhibitor V, 50 μM Akt inhibitor VII, or 24 μM Akt inhibitor IX; with 2 nM to 20 μM rapamycin or everolimus for 2–60 h. Trifluoperazine, promazine, triflupromazine, chlorpromazine, promethazine, mesoridazine, thioridazine, nortriptyline, pimozide, niguldipine, loperamide, and fluspirilene were all tested at 0.5, 1, and 5 μM. Phenoxazine, phenothiazine, and quinacrine were tested at 3 μM (higher concentrations were toxic). All experiments were repeated at least three times.

Western Blotting. Western blotting was performed as described (3, 6, 7). All experiments were performed at least three times with consistent results.

Semiquantitative Potency Studies. Striatal neurons from three litters were prepared, grown for 7 d, washed three times with medium without serum, and treated overnight with vehicle or 0.5, 1, or 5 μM compound. No significant death was observed. Neurons were washed, lysed, and blotted with LC3 antibody. Potency was defined as the ratio of LC3-II levels in treated neurons to LC3-II levels in control neurons, normalized to the actin loading control. Based on the drug's ability to induce autophagy, the compounds were semiquantitatively divided into five groups: (*i*) 10-NCP and trifluoperazine (strongest stimulators); (*ii*) promazine, promethazine, chlorpromazine, and triflupromazine; (*iii*) mesoridazine and thioridazine; (*iv*) niguldipine, loperamide, pimozide, and fluspirilene; and (*v*) nortriptyline (weakest stimulator).

GFP-LC3 Puncta Formation. Puncta formation was monitored as described (8). Experiments were repeated three times with cultures from different mouse litters. At least 20 transfected cells were analyzed in each experiment.

Electron Microscopy. Striatal neurons were cultured for 7–10 d as described above and treated with vehicle or 1 or 10 μM 10-NCP overnight. Cultures were fixed in an ice-cold solution of 2% glutaraldehyde, 1% paraformaldehyde, and 100 mM sodium cacodylate (pH 7.4), postfixed in 2% osmium tetroxide, block-stained in 2% aqueous uranyl acetate, dehydrated in acetone, and embedded in LX-112 resin (Ladd Research Industries). Ultrathin sections were contrast-stained with 0.8% lead citrate, examined with a JEM-1230 electron microscope (JEOL USA), and photographed with an Ultrascan USC1000 digital camera (Gatan). The ultrastructural criteria used to identify the organelles were as described (9, 10). Briefly, neurons were fixed and analyzed in an unbiased manner (i.e., every section of the cell has an equal probability of inclusion in the analysis). Autophagosomes were identified on the basis of the ribosome-free double membrane. The precursors were manifested by the layers of membranes. Mature double-membrane autophagosomes contained cytoplasm or mitochondria. Multilamellar membranous structures contained stacks of membranes and often mitochondria. Autolysosomes and lysosomes were identified as single-membrane structures filled with degraded or partly degraded material. Untreated and 10-NCP–treated neurons appeared healthy and intact, the cytoplasm had retained its integrity, and organelles (e.g., Golgi apparatus, endoplasmic reticulum, mitochondria) were not swollen or vacuolated.

Microscopy and Survival Analysis. Statistical analysis used Metamorph (Molecular Devices, CA), as described (2, 4), with cumulative hazard curves generated by Statview (Apple, CA). Striatal neurons expressing mutant Htt were transfected for 5–7 d in vitro with pGW1-GFP (survival marker) or both pGW1-mCherry and pGW1-Htt^{ex1}-Q72-GFP at a 1:1 molar ratio (2–3 μg of total DNA in each well of a 24-well plate). Neurons were treated with vehicle (DMSO) or with 1 or 10 μM 10-NCP 24 h after transfection and imaged immediately and then every 24 h for 1 wk. Fresh 10-NCP or DMSO was provided daily by changing the medium. Neurons that died during the imaging interval were assigned a survival time (the period between transfection and their disappearance from an image). These event times were used to obtain the cumulative risk for death graph, which was analyzed for statistical significance using the Mantel–Cox test. Experiments were repeated two to three times with more than 100 neurons per condition.

Image Analysis. Measurements of Htt expression and IB formation were extracted from files obtained by automated imaging. Expression of GFP-tagged Htt was estimated by measuring GFP fluorescence intensity over a region of interest corresponding to the neuronal soma (using the fluorescence of cotransfected mCherry as a guide to draw the region of interest). The intensity values were background-subtracted and normalized to those at time "zero." To control for potential changes in transcription or translation, the intensity of mCherry, which is expressed from the same plasmid as GFP-tagged Htt, was also measured.

The cumulative risk for IB formation in cohorts of neurons that asynchronously formed IBs was calculated with Statview. The time of IB formation after transfection was used as the event time variable.

Determining Expression Levels of GFP-Tagged Mutant Htt. To determine whether 10-NCP stimulates degradation of exogenous mHtt^{ex1}-GFP expressed at endogenous WT Htt levels, we estimated the degree of mHtt^{ex1}-GFP overexpression in our cultured neurons. We analyzed cohorts of neurons that express mutant Htt^{ex1}-Q72-GFP and identified neurons that expressed mutant Htt^{ex1}-GFP at approximately the same level as endogenous full-length Htt.

Rat striatal neurons were cultured as described above. Cultures were transfected with pGW1-Htt^{ex1}-Q72-GFP and fixed 24 h later. Neurons were fixed and stained with an antibody that recognizes amino acids 2–17 of Htt (Enzo Life Sciences) (7). Antibody staining was visualized with Cy3-conjugated secondary antibody. The levels of Htt antibody were determined in Htt^{ex1}-Q72-GFP–transfected cells (using GFP as a marker of transfected neurons) and in nontransfected cells (no GFP fluorescence). The signals from untransfected cells are $z = 2x$, and the signals from transfected neurons are $z = 2x + y$, where z is the overall signal, x is the signal attributable to each copy of WT Htt, and y is transfected Htt^{ex1}. This allowed us to identify the threshold signals of transfected Htt^{ex1} at approximately the same levels as endogenous full-length Htt. Knowing the threshold signals, we analyzed our original data for live neurons that express Htt^{ex1}-Q72-GFP at approximately the same levels as endogenous full-length Htt. 10-NCP lowered the Htt^{ex1}-Q72-GFP levels in the low-expressing neurons.

Pharmacophore Modeling. Pharmacophore modeling was performed with the Pharmacophore Protocol within Discovery Studio version 2.1 (Accelrys). Low-energy conformations of all the compounds reported in Fig. 3 were determined with the CHARMm force field within Discovery Studio version 2.1, using the default potentials.

1. Fung C, Lock R, Gao S, Salas E, Debnath J (2008) Induction of autophagy during extracellular matrix detachment promotes cell survival. *Mol Biol Cell* 19:797–806.
2. Arrasate M, Mitra S, Schweitzer ES, Segal MR, Finkbeiner S (2004) Inclusion body formation reduces levels of mutant huntingtin and the risk of neuronal death. *Nature* 431:805–810.
3. Rao VR, et al. (2006) AMPA receptors regulate transcription of the plasticity-related immediate-early gene Arc. *Nat Neurosci* 9:887–895.
4. Arrasate M, Finkbeiner S (2005) Automated microscope system for determining factors that predict neuronal fate. *Proc Natl Acad Sci USA* 102:3840–3845.
5. Mizushima N, Yamamoto A, Matsui M, Yoshimori T, Ohsumi Y (2004) In vivo analysis of autophagy in response to nutrient starvation using transgenic mice expressing a fluorescent autophagosome marker. *Mol Biol Cell* 15:1101–1111.
6. Mitra S, Tsvetkov AS, Finkbeiner S (2009) Single neuron ubiquitin-proteasome dynamics accompanying inclusion body formation in Huntington disease. *J Biol Chem* 284:4398–4403.
7. Brooks E, Arrasate M, Cheung K, Finkbeiner SM (2004) Using antibodies to analyze polyglutamine stretches. *Methods Mol Biol* 277:103–128.
8. Bradley J, Carter SR, Rao VR, Wang J, Finkbeiner S (2006) Splice variants of the NR1 subunit differentially induce NMDA receptor-dependent gene expression. *J Neurosci* 26:1065–1076.
9. Klionsky DJ, et al. (2008) Guidelines for the use and interpretation of assays for monitoring autophagy in higher eukaryotes. *Autophagy* 4:151–175.
10. Fengsrud M, et al. (1995) Ultrastructural and immunocytochemical characterization of autophagic vacuoles in isolated hepatocytes: Effects of vinblastine and asparagine on vacuole distributions. *Exp Cell Res* 221:504–519.

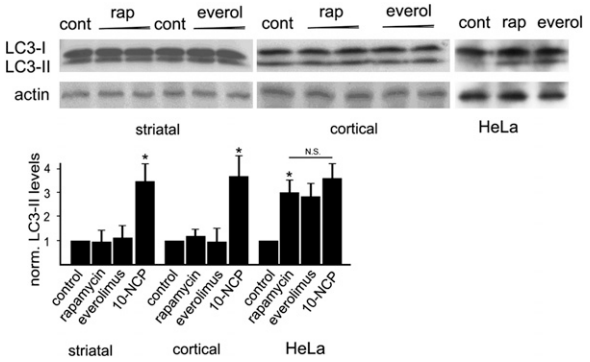

Fig. S1. 10-NCP induces neuronal autophagy better than other neuronal autophagy enhancers. The mTOR inhibitors rapamycin and everolimus have been well established as autophagy inducers in nonneuronal cells. Striatal and cortical neurons were incubated in medium with 2–20 μM rapamycin (rap) or 2–20 μM everolimus (everol) for 48 h. Shorter or longer incubations and higher and lower concentrations (2 nM to 20 μM) gave similar results. Rapamycin (2 μM, 24 h) induced autophagy in HeLa cells. The effect of 10-NCP was calculated from Fig. 1. Striatal, $*P < 0.001$ (ANOVA). Cortical, $*P < 0.001$ (ANOVA). HeLa, $P < 0.001$ (ANOVA).

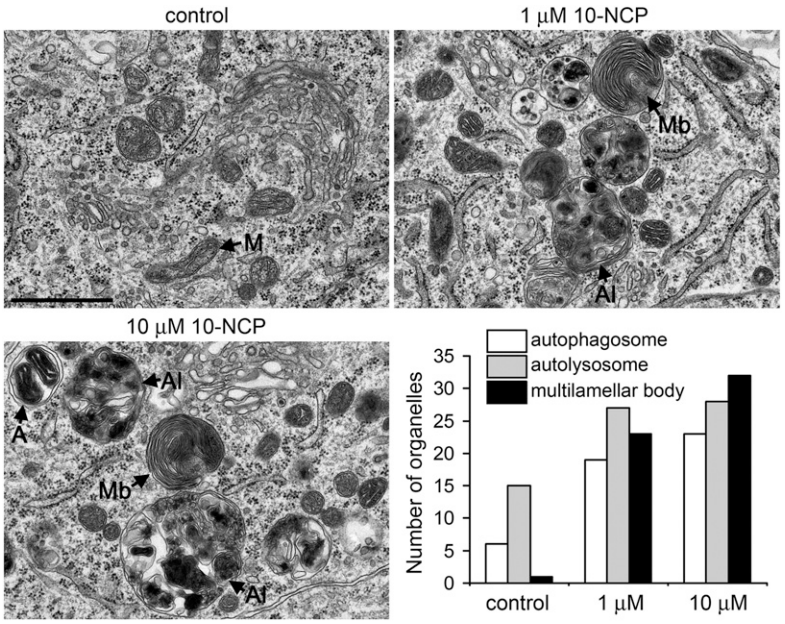

Fig. S2. Quantification of electron micrographs of striatal neurons treated with 10-NCP (0, 1, or 10 μM, overnight). A, autophagosomes; Al, autolysosome; M, mitochondria; Mb, multilamellar body. (Scale bar, 1 μm.) Microphotographs were analyzed in an unbiased manner (i.e., every section of the cell had an equal probability of inclusion in the analysis). Organelles were counted from these microphotographs.

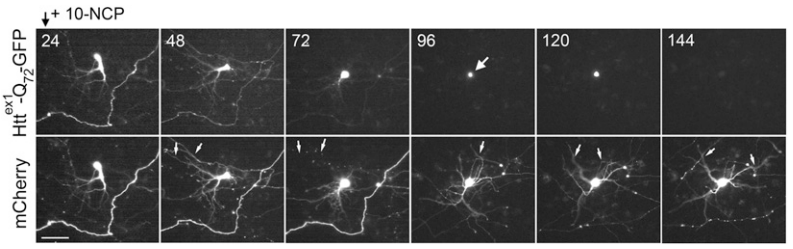

Fig. S3. Disappearance of an IB (large arrow) in a neuron treated with 10-NCP (1 μM) in the experiments in Fig. 2*C*. Note that neurite retraction is reversible. Neurites are marked with the small arrows. Numbers reflect hours after transfection. Neurons were treated with 10-NCP immediately after the first round of imaging. (Scale bar, 15 μm.)

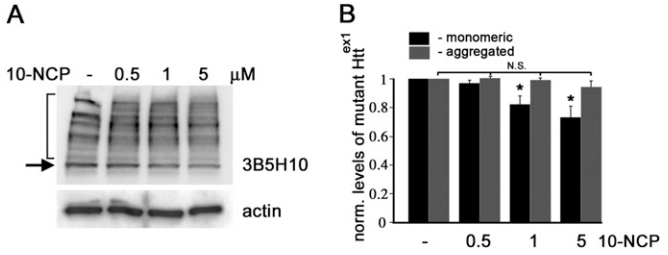

Fig. S4. 10-NCP decreases levels of transgenically expressed mutant Htt^{ex1} in cultured neurons from the R6/2 mice. (*A*) Striatal R6/2 neurons were treated overnight with 0.5, 1, and 5 μM 10-NCP. Membranes were incubated with 3B5H10 antibody, which recognizes an abnormal pathogenic polyglutamine stretch. The arrow indicates nonaggregated Htt^{ex1}, and the bracket indicates the aggregates. Actin was used as a loading control. (*B*) Quantification of four blots. $P < 0.001$ (ANOVA). norm, normalized; N.S., not significant.

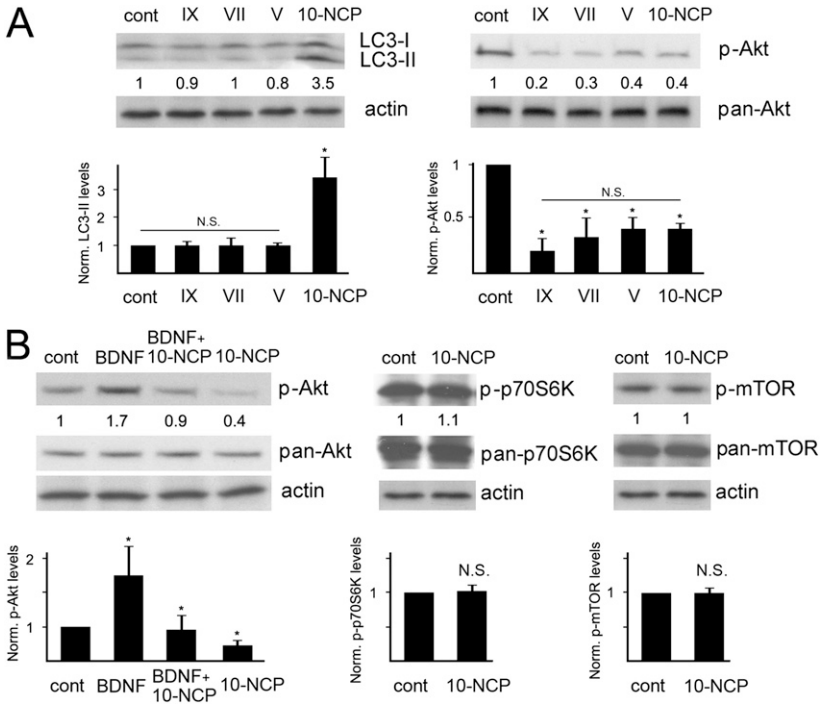

Fig. S5. 10-NCP induces autophagy in an Akt- and mTOR-independent fashion. (*A*) Akt inhibitors V, VII, and IX fail to induce neuronal autophagy [*Left*, $*P < 0.001$ (ANOVA)], even though they inhibit Akt activation at the doses used [*Right*, $*P < 0.01$ (ANOVA)]. This suggests that 10-NCP's autophagy-inducing effects are independent of its known inhibitory effects on Akt. 10-NCP was used as a control. Phospho-Akt levels are normalized to total Akt. cont, control; norm., normalized; N.S., not significant. (*B*) Treatment with 10-NCP (10 μM, 4 h) changes the levels of phosphorylated Akt in both stimulated and unstimulated striatal neurons. Stimulation was performed with 100 ng/mL BDNF overnight. $*P < 0.001$ (ANOVA). However, this same 10-NCP treatment did not change the normalized levels of phosphorylated mTOR and p70S6K, which are kinases downstream of Akt.

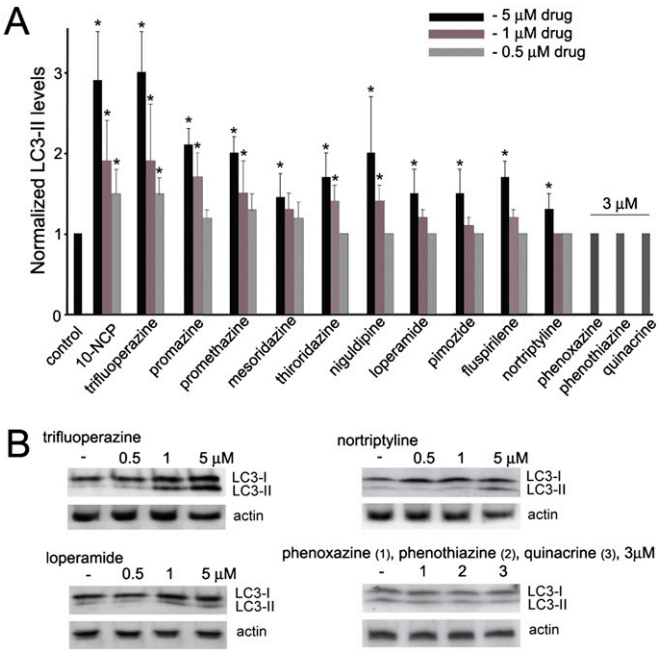

Fig. S6. A family of structurally related compounds induces autophagy in primary neurons. (*A*) Striatal neurons were treated overnight with each compound. No significant death was observed. Drug potency was assayed by using the levels of LC3-II induction for each compound at 0.5, 1, and 5 μM as a semi-quantitative readout. Phenoxazine, phenothiazine, and quinacrine were tested at 3 μM (higher concentration was toxic). Actin was used as a loading control. $*P < 0.01$ (*t* test: control and a treatment condition). (*B*) LC3 blots of trifluoperazine (0.5, 1, and 5 μM), nortriptyline (0.5, 1, and 5 μM), loperamide (0.5, 1, and 5 μM), phenoxazine (3 μM), and phenothiazine (3 μM).

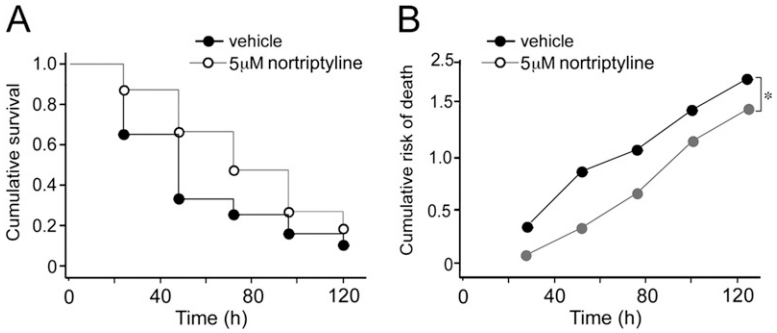

Fig. S7. Nortriptyline is protective in a neuronal model of HD. (*A*) Striatal neurons transfected with mCherry (a morphology and viability marker) and the amino-terminal exon 1 fragment of Htt^{ex1} containing a pathogenic stretch of 72 glutamines fused to the N terminus of GFP were treated with 5 μM nortriptyline, which led to a small reduction in cell death. Note that 5 μM nortriptyline is a weaker neuroprotectant than 1 μM 10-NCP (Fig. 2*B*), consistent with its weaker autophagy-inducing capacity (Fig. S6). (*B*) Cumulative risk for death associated with nortriptyline treatment calculated from the Kaplan–Meier curves in *A*. $*P < 0.001$ (Mantel–Cox test).

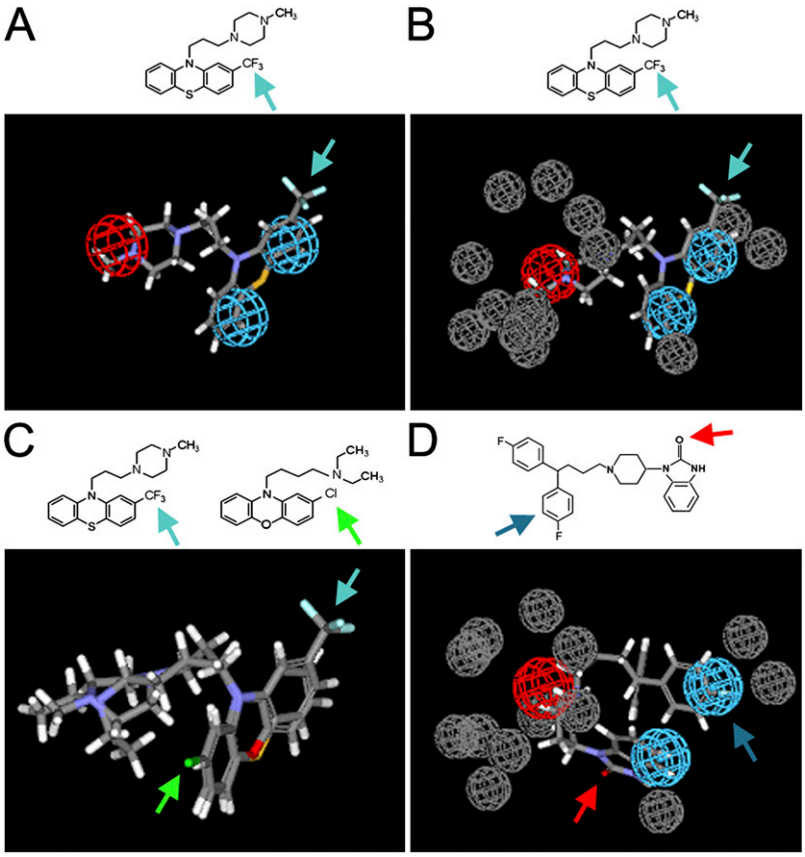

Fig. S8. Refined pharmacophore model explains the ranked potencies of tested autophagy-inducing compounds. The refined pharmacophore contains three positive chemical features—two hydrophobe aromatic spheres (blue) and a positive-charge sphere (red)—and 14 areas of ligand exclusion (gray). (*A*) Three-positive-feature pharmacophore fitted with trifluoperazine. The turquoise arrow facilitates orientation of the CF3 group. (*B*) Complete pharmacophore model (including 14 exclusion spheres) fitted with trifluoperazine. The turquoise arrow facilitates orientation of the CF3 group. (*C*) Superimposition of the best low-energy conformations of trifluoperazine and 10-NCP. The chlorine of 10-NCP (green arrow) is surprisingly located in a different area of space relative to the trifluoromethyl moiety of trifluoperazine (turquoise arrow). (*D*) Complete pharmacophore model (including 14 exclusion spheres) fitted with pimozide. Only one of the 4-fluoro-phenyl moieties (dark blue arrow) interacts with the hydrophobic aromatic feature (the other occupies a region outside the positive-feature space of the pharmacophore and away from any exclusion zone). The second hydrophobic aromatic interaction is made partially by the benzimidazole-2-one group (red arrow).